

Heat Capacity of Tetramethylsilane in the Region from 2 to 26 K and Premelting Range¹⁾

Takako SHINODA, Hisae ENOKIDO, Yoji MAEDA,* Hiroshi TOMITA, and Yo-ichiro MASHIKO

National Chemical Laboratory for Industry, Shibuya-ku, Tokyo

(Received April 26, 1972)

The heat capacity of tetramethylsilane was measured at temperatures from 2 to 26 K and in the premelting temperature range for two crystalline forms. There are two crystalline forms in solid tetramethylsilane. The heat of fusion and triple point temperature of a stable form were found to be 1611.2 ± 0.9 cal/mol and 174.049 K, while those of a metastable form to be 1396.0 ± 0.8 cal/mol and 170.981 K. Tetramethylsilane was highly purified by preparative gas chromatography. The amount of impurity in the specimen of $\text{Si}(\text{CH}_3)_4$ was estimated to be 0.004₈ mol% from measurement of the melting point range for two crystalline forms. The Debye characteristic temperature at 0 K, $\theta_D(0)$, was derived from low temperature heat capacity data, and the $\theta_D(T)/\theta_D(0)$ curve was compared with those for $\text{C}(\text{CH}_3)_4$ and CF_4 . Despite high purity, C_p values for two crystalline forms in the region below melting points increases abnormally with the rise of temperature. The phenomena were interpreted as due to effects of formation of vacancies in the crystals and of melting accompanied by molecular orientation transition; analysis of heat capacity curves for the two crystalline forms was made in the region below the melting point.

In previous papers^{2,3)} we reported on the thermodynamic properties of tetrahedral molecules, $\text{C}(\text{CH}_3)_4$ and CF_4 , which undergo orientationally disordering transition below their melting point. In the present paper we treat tetramethylsilane $\text{Si}(\text{CH}_3)_4$ which does not undergo phase transition below its melting point.

Heat capacity data for $\text{Si}(\text{CH}_3)_4$ were given by Aston *et al.*⁴⁾ In their work the sample used was of 99.88 mol% purity, and the heat capacity data were reported for temperatures 12 to 290 K. We have attempted to prepare $\text{Si}(\text{CH}_3)_4$ of higher purity, and provide more complete and accurate data on the heat capacity at lower temperatures and in the premelting range, supplementing the data for $T < 12$ K.

The Debye characteristic temperature at 0 K, $\theta_D(0)$, is derived from the low temperature heat capacity data, and a comparison of the temperature dependence of $\theta_D(T)/\theta_D(0)$ is made with that for other tetrahedral molecules reported by the present authors taking into account the octupole interaction of molecules in the crystals.

A possible interpretation of premelting anomalies in two crystalline forms of $\text{Si}(\text{CH}_3)_4$ is offered by theories of lattice vacancies and simultaneous positional and orientational transitions, and the activation energies are estimated from the analysis of the heat capacity curves in the region below melting point.

Experimental

Materials. Tetramethylsilane was obtained from Matheson Coleman & Bell Co. In analytical experiments, a Shimadzu 4AT gas chromatograph was used with a thermal conductivity detector under the following conditions:

* Present address: Research Institute for Polymers & Textiles, Sawatari, Kanagawa-ku, Yokohama, Japan.

1) Presented at the 23rd Annual Meeting of the Chemical Society of Japan, Tokyo, April, 1970.

2) H. Enokido, T. Shinoda, and Y. Mashiko, *This Bulletin*, **42**, 84 (1969).

3) H. Enokido, T. Shinoda, and Y. Mashiko, *ibid.*, **42**, 3415 (1969).

4) J. G. Aston, R. M. Kennedy, and H. G. Messerly, *J. Am. Chem. Soc.*, **63**, 2343 (1941).

Column 3 mm \times 3 m, Silicone SE 30 (20%) on Shimalite W (80—100 mesh)

Temperature 30°C

Carrier gas Helium at 40 ml/min.

A chromatogram of crude $\text{Si}(\text{CH}_3)_4$ is shown in Fig. 1. Retention times and percentage composition of crude $\text{Si}(\text{CH}_3)_4$ are shown in Table 1. The percentage composition was calculated by means of area under peaks.

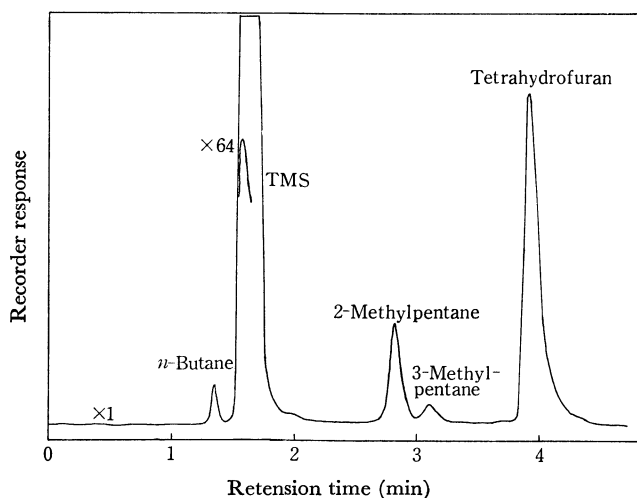


Fig. 1. Analytical gas chromatogram of crude $\text{Si}(\text{CH}_3)_4$.

TABLE 1. RETENTION TIMES AND PERCENTAGE COMPOSITION OF CRUDE $\text{Si}(\text{CH}_3)_4$

Components		Retention time (min)	Calculated composition (%)
Peak No.	Compound		
1	<i>n</i> -Butane	1.3	0.02
2	Tetramethylsilane	1.6	98.12
3	2-Methylpentane	2.8	0.29
4	3-Methylpentane	3.1	0.03
5	Tetrahydrofuran	3.8	1.52

Attempts to remove impurities by a fractional distillation or zone refining were unsuccessful, but they were completely removed by preparative scale gas chromatography. A Varian Aerograph Autoprep 712 preparative instrument with a hydrogen flame ionization detector was used to prepare a

total of 100 ml of pure $\text{Si}(\text{CH}_3)_4$ under the following conditions:

Column	3/8 in (O.D.) \times 50 ft Silicone SE 30 (10%) on Chromosorb A (60–80 mesh)
Temperature	80°C
Carrier gas	Nitrogen at 150 ml/min.
Sample size	2.0 ml injected manually

No impurities of the collected $\text{Si}(\text{CH}_3)_4$ were detected by analytical gas chromatography. However, the amount of solid-insoluble liquid-soluble impurity was determined by the measurement of melting point, the purity being found to be 99.995₄ mol%.

Apparatus. A new calorimeter was constructed to measure the heat capacity of substances which are solid or liquid at room temperature in the range from 2 K to 150°C. In basic design the cryostat is similar to the adiabatic calorimeter for condensed gases described previously.⁵⁾ The general assembly is illustrated in Fig. 2. About three liters of liquid helium can be held by a coolant container F (brass cylinder) which allows measurement to continue for a period longer than 12 hours at low temperature. A thermal station E (copper cylinder) has an internal volume of about 500 cc, and can contain liquid helium in the measurements at low temperature. A heater (#34 manganin) is wound around E, and a difference thermocouple is placed between the thermal station and the top of an adiabatic shield B. Thermocouple junctions (chromel p—constantan) are provided at the bottom of F and at E for their absolute temperature measurements. All electrical lead wires come from the top of the cryostat through a stainless steel pipe at the center. They wound round the cylinder at the bottom of F and also round E and B, entering inside the shield through 30 holes drilled at the bottom edge of the side of the adiabatic shield. In assembly, an inside jacket G is soldered to the bottom of F and an outside jacket H to the top plate both with Wood's alloy or solder.

A sectional view of the calorimeter vessel, made of silver-plated copper (0.2 mm thick) and with an internal volume of about 60 cc, is shown in Fig. 3. It is hung by means of

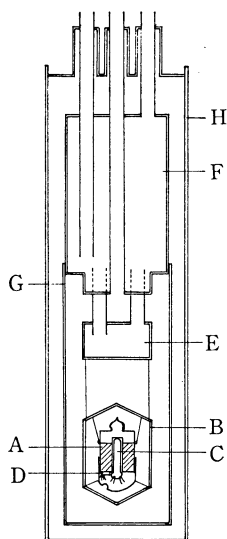


Fig. 2. Cross-section diagram of the cryostat.

A: calorimeter vessel, B: adiabatic shield, C: platinum thermometer, D: germanium thermometer, E: thermal station, F: coolant container, G: inside jacket, H: outside jacket.

nylon cords within the adiabatic shield. Eight vanes are soldered inside the vessel. The cap of the vessel is made of Kovar and attached to a Pyrex glass tube through which the vessel can be evacuated and sealed in a vacuum. A platinum thermometer with a heater (#34 manganin, 65 Ω) wound on it is cast into a re-entrant well with Wood's alloy. A germanium thermometer is attached to the bottom of the vessel by means of a sheath (copper). The platinum resistance thermometer used above 13.5 K had been calibrated at the National Bureau of Standards (J. L. Riddle, 1959). The temperature scale was re-calculated on the International Practical Temperature Scale of 1968 by using the tables of differences between the NBS-55 scale, the IPTS-48 and the IPTS-68 derived by Douglas⁶⁾ and Bedford *et al.*⁷⁾ The germanium resistance thermometer (Cryocal, Inc.) which had been calibrated on the thermodynamic scale at the NBS (Jacquelyn A. Wise, 1969) was used in the temperature range below 13.5 K. All measuring operations of the heat input and the resistances of the thermometers were manually carried out. The monitoring and control of adiabatic conditions were automatically made.²⁾

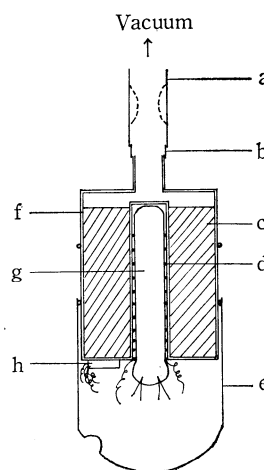


Fig. 3. Cross-section diagram of calorimeter vessel.

a: Pyrex glass tube, b: Kovar tube, c: vane, d: manganin heater, e: copper sheath, f: silver-plated copper vessel, g: platinum thermometer, h: germanium thermometer.

Results and Discussion

Heat Capacity of $\text{Si}(\text{CH}_3)_4$. The amount of sample in the calorimeter was determined to be 23.0475 g (=0.261233 mol, 35 cc) as liquid by measuring the filling weight. The measured values of heat capacity in the region 2–26 K and in the premelting range are listed in Table 2. Corrections were made for curvature where necessary. At low temperature, temperature increments were about 0.3–1°. These increased to about 2° at higher temperature. The measurements of heat capacity below melting point were also made several times with various small temperature rise (0.1–0.8°) to determine detailed shapes of heat capacity curves for two crystalline forms in the premelting region. Equilibrium time after heating varied from less than one minute at low temperature to about 7–8 min at higher temperature. In the

6) T. B. Douglas, *J. Res. NBS*, **73A** 451 (1969).

7) R. E. Bedford, M. Durieux, R. Muijlwijk, and C. R. Barver, *Metrologia*, **5**, 47 (1969).

5) T. Shinoda, T. Atake, H. Chihara, Y. Mashiko, and S. Seki, *Kogyo Kagaku Zasshi*, **69**, 1619 (1966).

TABLE 2. HEAT CAPACITY OF $\text{Si}(\text{CH}_3)_4$
(Molecular weight 88.226; 1 cal=4.1840 absolute joules; $0^\circ\text{C}=273.15\text{ K}$)

$T(\text{K})$	C_p (cal/deg mol)	$T(\text{K})$	C_p (cal/deg mol)	$T(\text{K})$	C_p (cal/deg mol)	$T(\text{K})$	C_p (cal/deg mol)
(Stable form)		12.568	1.095	129.930	26.95	167.726	32.94
2.178	0.004609	12.699	1.127	131.739	27.19	168.747	33.24
2.211	0.005407	13.235	1.269	131.891	27.23	169.761	33.70
2.378	0.005865	13.418	1.321	132.842	27.39	170.764	34.21
2.758	0.008470	14.007	1.474	133.834	27.53	171.581	35.02
3.104	0.01149	14.174	1.524	134.903	27.69	171.753	35.14
3.111	0.01112	15.037	1.793	135.909	27.86	172.441	36.93
3.462	0.01563	15.637	1.977	136.686	27.98	173.193	49.69
3.685	0.01862	15.900	2.056	136.946	28.06	(Metastable form)	
3.822	0.02022	16.520	2.259	137.964	28.20	136.092	28.44
4.104	0.02649	16.828	2.354	138.971	28.36	138.103	28.80
4.165	0.02739	17.371	2.532	140.000	28.51	140.117	29.13
4.478	0.03380	17.803	2.676	140.679	28.60	142.110	29.49
4.673	0.03953	18.288	2.837	140.978	28.64	144.155	29.78
4.804	0.04296	18.488	2.888	141.025	28.66	146.223	30.13
5.068	0.05152	19.243	3.154	142.730	28.91	148.252	30.46
5.121	0.05318	19.643	3.293	142.969	28.96	150.261	30.76
5.454	0.06620	20.146	3.451	144.714	29.22	152.249	31.11
5.470	0.06675	20.869	3.696	144.945	29.25	154.488	31.45
5.814	0.08241	21.019	3.755	146.747	29.53	156.501	31.76
5.880	0.08547	21.915	4.046	148.832	29.85	158.496	32.10
6.194	0.1025	22.196	4.144	150.345	30.08	160.474	32.45
6.292	0.1080	22.784	4.336	151.143	30.21	161.980	32.72
6.583	0.1269	23.491	4.566	152.388	30.39	163.025	32.93
6.700	0.1348	24.202	4.807	153.188	30.53	164.008	33.13
6.982	0.1558	24.666	4.950	155.045	30.81	164.938	33.35
7.111	0.1660	25.142	5.098	155.215	30.84	165.864	33.58
7.385	0.1901	25.749	5.289	157.049	31.13	166.584	33.89
7.522	0.2027	26.023	5.371	157.227	31.18	167.555	34.81
7.788	0.2283	105.995	23.29	159.058	31.42	168.506	36.07
7.939	0.2453	107.960	23.61	159.221	31.46	168.891	36.34
8.196	0.2732	109.905	23.92	159.803	31.52	169.420	39.11
8.364	0.2938	111.822	24.21	159.896	31.53	170.200	57.12
8.613	0.3243	113.764	24.51	161.200	31.71	170.294	89.21
8.792	0.3485	115.730	24.83	161.491	31.77	(Liquid)	
9.232	0.4117	117.756	25.14	162.238	31.90	172.372	38.95
9.665	0.4808	119.839	25.47	162.910	32.00	172.895	39.06
10.076	0.5528	121.898	25.78	163.269	32.06	173.939	39.07
10.333	0.6035	123.935	26.07	164.268	32.26	174.793	39.12
10.855	0.7014	125.952	26.36	165.320	32.46	175.985	39.23
11.832	0.9153	127.861	26.66	165.566	32.50	176.078	39.27
11.849	0.9205	127.951	26.67	166.702	32.74	177.448	39.33

vicinity of melting point and for the melting duration, it became about 14—30 min. We observed heat capacity anomaly to have a very large value (*i.e.* 49.69 cal/mol deg at 173.193 K for a stable form, and 135.4 and 308.7 cal/mol deg at 170.623 and 170.776 K for a metastable form). No hysteresis was observed.

Triple Points of Two Crystalline Forms of $\text{Si}(\text{CH}_3)_4$. When a sample of $\text{Si}(\text{CH}_3)_4$ is cooled from room temperature, it crystallizes in a metastable form and is then transforms into a stable form. The transition temperature is dependent upon the cooling rate.

The triple point of each form was obtained from a plot of equilibrium temperatures against reciprocals of the fraction melted. The result is summarized in Table

3. The triple point temperature for the sample of the stable form of $\text{Si}(\text{CH}_3)_4$ was found to be 174.049 K, and that of the metastable form 170.981 K. The values are also compared with those given by Aston *et al.* in Table 3.

Heats of Fusion of Two Crystalline Forms of $\text{Si}(\text{CH}_3)_4$. Data of the heat of fusion for the two crystalline forms are summarized in Table 4 together with those obtained by Aston *et al.* The agreement is not very good, being beyond assigned uncertainties. This is probably due to the fact that it is difficult to estimate exactly a $\int C_p dT$ correction at temperatures slightly below melting point, because C_p value in the premelting range increases unusually with temperature, despite high purity of the

TABLE 3. THE TRIPLE POINT OF Si(CH₃)₄
Stable Form

Fraction melted	<i>T</i> (K)
0.18344	174.041
0.23787	174.044
0.32486	174.046
0.49740	174.047
<i>T</i> _{triple} (pure)	174.049
Aston <i>et al.</i> (1941)	174.12±0.05

Metastable Form	
Fraction melted	<i>T</i> (K)
0.18814	170.973
0.24459	170.975
0.32934	170.977
0.50451	170.979
0.93006	170.981
<i>T</i> _{triple} (pure)	170.983
Aston <i>et al.</i> (1941)	171.04±0.05

TABLE 4. HEAT OF FUSION OF Si(CH₃)₄

Temperature interval (K)	Heat input (cal/mol)	∫ <i>C_p</i> <i>dT</i> (cal/mol)	Δ <i>H</i> (cal/mol)
(mol wt 88.226; 0.261233 mol)			
Stable Form			
173.597—174.232	1665.4	53.3	1612.1
173.567—175.253	1728.0	117.7	1610.3
		average	1611.2±0.9
Aston <i>et al.</i> (1941)			1648.0±3.5
Metastable form			
170.827—172.234	1499.6	102.8	1396.8
170.548—171.529	1454.3	59.1	1395.2
		average	1396.0±0.8
Aston <i>et al.</i> (1941)			1426.8±0.3

sample.

Heat Capacities of Two Crystalline Forms in the Premelting Range. Heat capacities of both crystalline form of Si(CH₃)₄ showed marked upward trends in the temperature region below their melting points as seen in Fig. 4. This behavior might be due to effects of impurity in the sample, lattice vacancy formation and simultaneous positional and orientational transitions. An attempt was made to interpret the premelting anomalies for the two crystalline forms by ascribing to several causes.

The effect on heat capacity induced by impurities was estimated from the purity determined in the previous section. By the same treatment as in the analysis for neopentane,²⁾ the formulas of normal heat capacity in the region below melting point are given in the following:

$$C_p(\text{normal}) = 7.206 + (0.15208)T \quad (1)$$

for a stable form,

$$C_p(\text{normal}) = 6.383 + (0.16232)T \quad (2)$$

for a metastable form. Normal heat capacities of both crystalline forms estimated by means of formulas (1) and (2) in the region below melting points are shown

by dashed curves in Fig. 4. It can be assumed that excess heat capacity Δ*C_p* remaining after subtracting *C_p* (impurity) and *C_p* (normal) from the total, is caused by thermal creation of imperfections. If we assume Schottky-type vacancies, excess heat capacity due to vacancy formation *C*(vac.) is given by

$$C(\text{vac.}) \simeq (N) \exp(s_v/k)(1/k)(h_v/T)^2 \exp(-h_v/kT), \quad (3)$$

where *N* is Avogadro's number, *s_v* and *h_v* entropy and enthalpy, respectively, of vacancy formation, and *k* Boltzmann's constant. If ln(Δ*C_p* × *T*²) is plotted against 1/*T*, a straight line should be obtained, and the enthalpy of formation of vacancies can be estimated from its slope. Plots of log₁₀(Δ*C_p* × *T*²) versus 1/*T* for two crystalline forms of Si(CH₃)₄ are shown in Fig. 5.

The slope for the stable form gives *h_p* = 28 kcal/mol, and the plot for the metastable form gives two slopes (*h_p* = 30 and 47 kcal/mol). These values are too great

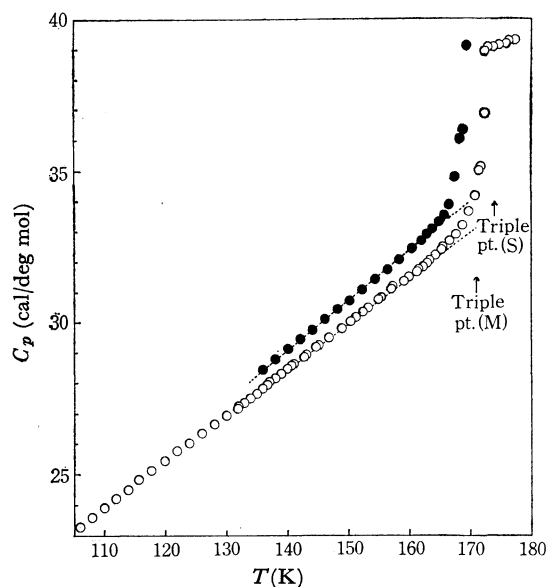


Fig. 4. Heat capacity of two crystalline forms in the premelting range.

○: Stable form ●: Metastable form ---: *C_p*(normal)

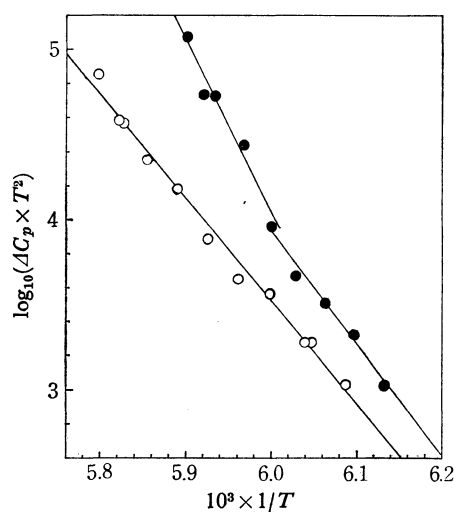


Fig. 5. Plot of log₁₀(Δ*C_p* × *T*²) versus 1/*T* for two crystalline forms of Si(CH₃)₄.

○: Stable form ●: Metastable form

and unreasonable for the enthalpy of formation of vacancies as compared with the value of 3240 ± 220 cal/mol obtained for neopentane. We attempted to interpret these values by assuming that $\text{Si}(\text{CH}_3)_4$ undergoes simultaneous positional and orientational transitions at melting point. According to a statistical treatment⁸⁾ of Ising lattice of three dimensions in terms of a series expansion method, the tail of heat capacity at sufficiently low temperature is given by the first term of low-temperature expansion:

$$C(\text{trans.}) \simeq (1/k)(E/T)^2 \exp(-E/(kT)), \quad (4)$$

where E corresponds to total (positional and orientational) energies of molecular interaction. It was also found by Aston *et al.*³⁾ that the height of potential barrier hindering internal rotation of methyl groups was considerably lower than that of neopentane. Thus, the values obtained may be regarded as the summation of the enthalpy of vacancy formation and the total energies of positional and orientational disordering of the molecules and internal rotation of methyl groups. However, it is very difficult to estimate each value from the summation without some information on crystal structure and molecular motions in the two forms of $\text{Si}(\text{CH}_3)_4$.

The calculation of the difference in entropy of metastable and stable forms at 170.981 K is summarized in Table 5. If the metastable form is cooled, it is transformed into the stable form with heat evolution. The entropy of transition is equal to the difference in the entropies of metastable and stable forms at transition temperature.

TABLE 5. ENTROPY DIFFERENCE BETWEEN METASTABLE AND STABLE FORMS OF $\text{Si}(\text{CH}_3)_4$

	ΔS (e.u.)
Liquid from 174.049 to 170.981 K	-0.693
Crystallization of Metastable Form	-8.165
	-8.858
Crystallization of Stable Form	-9.257
Stable Solid from 174.049 to 170.981 K	-0.663
	-9.920
$S_{\text{stable}} - S_{\text{metastable}}$ at 170.981 K	-1.062

Low Temperature Heat Capacity of $\text{Si}(\text{CH}_3)_4$

Figure 6 gives a graph of heat capacity measurement for solid $\text{Si}(\text{CH}_3)_4$ expressed in the form C_p/T^3 versus T^2 . In the region $T^2 < 10$ (i.e., $T < 3.1$ K), the experimental value of C_p/T^3 increases sharply as T decreases. The situation resembles that of CD_4 crystal in the region $T < 20$ K reported by Colwell *et al.*⁹⁾ The anomalous shape of the graph of C_p/T^3 versus T^2 may be accounted for by a certain amount of crystalline disorder, removal of the spatial degeneracy by crystalline field, isotope effects of partially deuterated methyl groups and some experimental errors. However, it does not seem worthwhile to do any analysis of heat capacity at this stage without further evidence.

If we are to describe the extra contribution to heat capacity as a Schottky-type anomaly, the heat capacity

may be separated into a T^{-2} term and normal lattice terms. In a graph of $C_p \times T^2$ versus T^5 , the intercept is the coefficient of extra contribution in T^{-2} to the heat capacity. The value 0.0051052 was used for the coefficient derived from the heat capacity data. The calculated $(C_p - 0.0051052)/T^3$ values are shown as a dashed curve in Fig. 6. This curve continues to decrease and approaches a constant value asymptotically, as shown in usual crystals. The constant value obtained corresponds to the Debye characteristic temperature of $136.8 \pm 2.0^\circ$ at 0 K, $\theta_D(0)$. In order to compare the temperature dependence of $\theta_D(T)$ assuming $6N$ degrees of freedom for $\text{Si}(\text{CH}_3)_4$ with those for $\text{C}(\text{CH}_3)_4$ and CF_4 , the values of $\theta_D(T)$ were plotted against temperature on a reduced scale using the $\theta_D(0)$, as shown in Fig. 7. Here the mean intramolecular rotational frequency of the methyl group in $\text{Si}(\text{CH}_3)_4$, 170.5 cm^{-1} , obtained by Durig *et al.*¹⁰⁾ from their far-infrared spectrum, was used and $C_p - C_v$ correction was neglected. In Fig. 7 the shape of the $\theta_D(T)/\theta_D(0)$ curve for $\text{Si}(\text{CH}_3)_4$ is rather similar to that for $\text{C}(\text{CH}_3)_4$ and CF_4 , although there are differences in detail. This seems to demonstrate that the $\text{Si}(\text{CH}_3)_4$ crystal does not differ from a tetrahedral plastic crystal. Only its transition point of orientational disordering is very close to melting point as observed in the pre-melting phenomena in the heat capacity curve.

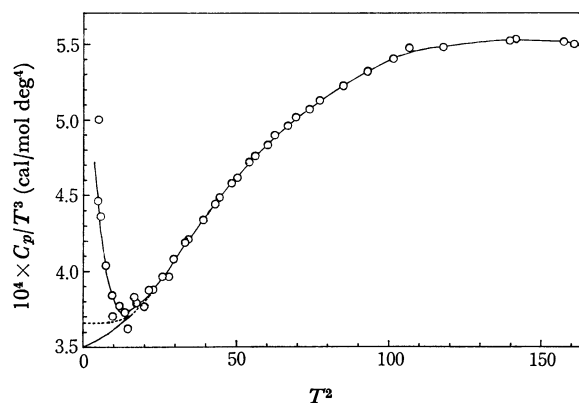


Fig. 6. Plot of C_p/T^3 versus T^2 for $\text{Si}(\text{CH}_3)_4$.

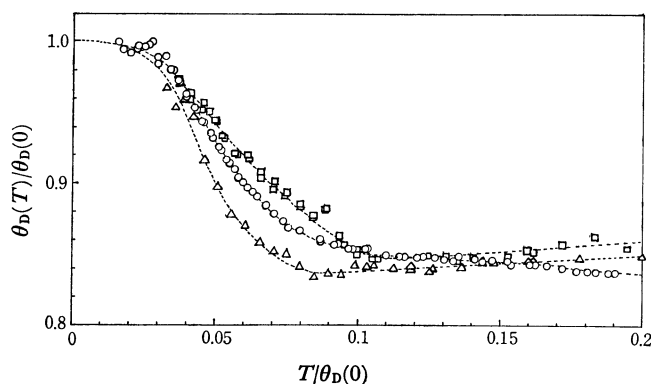


Fig. 7. $\theta_D(T)$ curve on a reduced basis of tetrahedral molecules

○: $\text{Si}(\text{CH}_3)_4$ ●: $\text{C}(\text{CH}_3)_4$ △: CF_4

9) J. H. Colwell, E. K. Gill, and J. A. Morrison, *J. Chem. Phys.*, **39**, 635 (1963).

10) J. R. Durig, S. M. Craven, and J. Bragin, *J. Chem. Phys.*, **52**, 2046 (1970).

8) C. Domb, *Advan. Phys.*, **9**, 289 (1960).